Journal of Inflammation Research

Dovepress
Taylor & Francis Group

Open Access Full Text Article

ORIGINAL RESEARCH

Eleutheroside E Attenuates Hypobaric Hypoxia-Induced High Altitude Pulmonary Edema by Regulating Ferritinophagy-Mediated Ferroptosis via Keap1-Nrf2 Regulatory Axis

Yilan Wang[1,*], Nan Jia[1,*], Zherui Shen[2], Sijing Zhao[1], Caixia Pei[1], Demei Huang[1], Zhenxing Wang[1]

[1]Hospital of Chengdu University of Traditional Chinese Medicine, Chengdu, People's Republic of China; [2]Chengdu University of Traditional Chinese Medicine, Chengdu, People's Republic of China

*These authors contributed equally to this work

Correspondence: Yilan Wang, Hospital of Chengdu University of Traditional Chinese Medicine, Chengdu, People's Republic of China, Email wangyilan@stu.cdutcm.edu.cn

Background: Eleutheroside E is a natural lignan and high-altitude pulmonary edema (HAPE) is a noncardiogenic pulmonary edema induced by exposure to a high-altitude environment. The present study is designed to investigate the therapeutic effects of eleutheroside E against HAPE in rats.

Methods: In this study, Sprague–Dawley rats were placed in a hypobaric hypoxia chamber (simulated altitude of 6,000 m; partial pressure of oxygen: 9.6 kPa) for 48 h of continuous exposure and treated with varying doses of eleutheroside E to evaluate its therapeutic effects against HAPE. To investigate the mechanism by which eleutheroside E regulates ferritinophagy and ferroptosis via the Keap1–Nrf2 axis, rescue experiments were performed using the autophagy inhibitor 3-MA, the ferroptosis agonist RSL3, and the Nrf2 inhibitor ML385. The therapeutic effects were validated by utilizing hematoxylin and eosin (H&E) staining, arterial blood gas analysis, lung wet/dry weight ratio, and inflammation cytokines. Furthermore, ferritinophagy-mediated ferroptosis was detected by transmission electron microscope, immunofluorescence staining, and Western blotting. Oxidative stress was detected by associated kits and reactive oxygen species levels.

Results: The administration of eleutheroside E alleviated HAPE in rats, and it could correct hypoxia and suppress lipid oxidation induced by hypobaric hypoxia. Moreover, it decreased the levels of inflammation cytokines, VEGF, and total proteins in the bronchoalveolar lavage fluid of rats. Autophagy was found to be involved in the pathological process of HAPE, specifically in the form of ferritinophagy, which represents a novel type of autophagy. The anti-ferritinophagy-mediated ferroptosis effects of eleutheroside E were confirmed by using transmission electron microscopy and Western blotting. The involvement of the Keap1-Nrf2 axis in eleutheroside E-mediated inhibition of ferritinophagy-driven ferroptosis was confirmed by rescue experiments.

Conclusion: In summary, eleutheroside E exhibits therapeutic effects against HAPE in rats by suppressing ferritinophagy-mediated ferroptosis via the Keap1-Nrf2 axis. This study indicated a prospective role of eleutheroside E as a functional component in preventing HAPE.

Keywords: eleutheroside E, high altitude pulmonary edema, autophagy, ferritinophagy, ferroptosis

Introduction

High altitude pulmonary edema (HAPE) is a rapidly progressive and severe condition which commonly occurs in lowlanders ascending to high altitudes. HAPE presents within 2–5 days of arrival at altitudes above 2500 m.[1] The incidence of HAPE is estimated at around 0.01% in a general mountaineering population at altitudes greater than 2000 m.[2] The prevalence of HAPE in climbers who ascend to more than 4000 m is 0.49%.[3] In most cases, symptoms of

https://doi.org/10.2147/JIR.S577574
Received: 4 November 2025
Accepted: 29 April 2026
Published: 5 May 2026

HAPE include fatigue, cough, dyspnea, and cyanosis. The treatment consists of rest, immediate improvement of oxygenation, nifedipine, phosphodiesterase inhibitors, dexamethasone, and acetazolamide.[4]

Nuclear erythroid-2-related factor 2 (Nrf2) plays a crucial role in regulating the cellular defense system against oxidative stress and maintaining cellular iron homeostasis.[5] Under normal state, the Nrf2 binds with Kelch-like ECH-associated protein 1 (Keap1) in the cytosol. The Nrf2/Keap1 signaling pathway was involved in the regulation of oxidative stress, inflammation, and apoptosis induced by acute hypoxia.[6] Activation of Nrf2 has the potential to mitigate hypobaric hypoxia-induced retinal apoptosis by effectively suppressing oxidative stress.[7] Reduced expression of Keap1 can promote the translocation of Nrf2 into the nucleus, thereby facilitating the expression of its target genes in cardiomyocyte injury induced by acute hypoxia.[8] Hence, it is reasonable to consider the Keap1/Nrf2 pathway as a potential candidate for addressing high-altitude illness through its capacity to elicit antioxidant responses.

Ferroptosis is a type of regulated cell death.[9] Multiple mechanisms involving ferroptosis have been reported in hypoxia-related diseases, including mitochondrial damage, formaldehyde accumulation, transcriptional regulation by hypoxia-inducible factors, iron metabolism disorders, and antioxidant imbalances.[10–15] Notably, a recent proteomic study revealed significant enrichment of the ferroptosis pathway in lung tissues from a high-altitude hypoxic acute lung injury model, accompanied by decreased GPX4 and SLC7A11 expression, iron accumulation, and increased lipid peroxidation.[16] Furthermore, iron bioavailability has been shown to play a critical role in high-altitude lung injury, as iron chelation exacerbates pulmonary edema while iron supplementation confers protection in rats exposed to simulated altitude of 6,000 meters.[17] In the context of pulmonary barrier integrity, studies in sepsis-induced lung injury have demonstrated that ferroptosis contributes to microvascular endothelial barrier disruption by downregulating tight junction proteins such as ZO-1 and occludin, and that inhibition of ferroptosis preserves endothelial integrity.[18]

Nuclear receptor coactivator 4 (NCOA4) directly interacts with the surface of ferritin and subsequently transports the ferritin complex to autophagosomes for lysosomal degradation, leading to iron release and promoting ferroptosis.[19] Iron derived from autophagy-mediated ferritin degradation induces cardiomyocyte death, accompanied by overexpression of NCOA4 and reactive oxygen species (ROS) accumulation.[20,21] Autophagy-dependent ferroptosis, as a distinctive cell death process, has been implicated in a multitude of diseases, whereas no research elucidates the relationship between autophagy-dependent ferroptosis and HAPE pathogenesis.

Eleutheroside E is a natural lignan isolated from *Eleutherococcus senticosus*. Eleutheroside E reportedly exhibits anti-inflammatory, anti-stress, antioxidant, and immunomodulatory properties. A study suggested that eleutheroside E prevented high-altitude heart injury and inhibited inflammation and pyroptosis via the NLRP3/caspase-1 signaling pathway.[22] The use of eleutheroside E significantly decreased intracellular ROS generation induced by high glucose and prevented the activation of the NF-κB signaling pathway.[23] Herein experiments were performed to address the role of the Keap1-Nrf2 axis in regulating HAPE-induced ferritinophagy-mediated ferroptosis, and investigated the functional impact of eleutheroside E in HAPE.

Materials and Methods

Reagents

3-MA (S2767), RSL3 (S8155), ML385 (S8790), and dexamethasone (S1322) were purchased from Selleck (Houston, Texas, US). Eleutheroside E (HPLC≥99.2%, A0254) was provided by Chengdu Must Bio-technology Co., Ltd. (Chengdu, Sichuan, China). The enzyme-linked immunosorbent assay (ELISA) kits for malondialdehyde (MDA), GSH, 4-hydroxynonenal (4-HNE), interleukin-6 (IL-6), tumor necrosis factor-α (TNF-α), tissue iron levels, and vascular endothelial growth factor (VEGF) were obtained from Nanjing Jiancheng (Nanjing, Jiangsu, China). The ROS determination kit (S0033M) was obtained from Beyotime Biotechnology (Shanghai, China) and used to measure ROS in rat lung tissues. Antibodies targeting β-actin, HIF-1α, AQP1, AQP4, GPX4, Nrf2, SQSTM1, NCOA4, and HO-1 were provided by Abcam (Cambridge, UK). Antibodies targeting TFRC, Keap1, and SLC7A11 were obtained from Abclonal Co., Ltd. (Wuhan, China). Antibodies targeting FTH1 were purchased from CST Inc. (Danvers, MA, US). Blood-gas analysis was performed using blood-gas test strips purchased from EPOC, Siemens Healthcare (Ottawa, Canada).

Animals

Male Sprague Dawley rats (seventy, weighing approximately 160–180 g, 6-week-old) were obtained from Dashuo Co., Ltd. (Chengdu, China). All rats were fed adaptively for one week before experiments (12 hours light/dark cycle, temperature: 20± 2 °C, humidity: 55 ± 5%, standard specific-pathogen-free conditions, standard pellet diet, and water ad libitum). The study protocol was approved by the Ethics Committee of Chengdu University of Traditional Chinese Medicine (Grant No. 2022–18). The experiments were executed according to the ARRIVE guidelines and were performed in strict adherence to the National Institutes of Health Guide for the Care and Use of Laboratory Animals.

Experimental Design

In the first part of the research, we evaluated the potential efficacy of eleutheroside E on high-altitude pulmonary illness. Forty-two rats were randomly divided into six groups of seven animals: normoxia control group (NC), eleutheroside E group (EE, 100 mg/kg), hypobaric hypoxia model group (HHM), eleutheroside E 50 group (EE 50, 50 mg/kg), eleutheroside E 100 group (EE 100, 100 mg/kg) and dexamethasone group (Dex, 4 mg/kg). The selection of the dexamethasone and eleutheroside E doses was determined based on the published scientific literature.[24,25] The implemented HAPE model was previously described.[26] Rats in the EE, EE 50, EE 100 and Dex groups received intraperitoneal drugs (once daily for three consecutive days). The NC and HHM groups were intraperitoneally injected with an equivalent volume of saline, at an injected volume of 5 mL/kg. After injections, rats in the HHM, EE50, EE100, and Dex groups were placed in a large environmental cabin (ProOx-830, Shanghai Tawang Intelligent Technology Co., Ltd). The duration of exposure in the hypobaric hypoxia chamber was 48 hours. The condition was set to a simulated altitude of 6000 m with an oxygen partial pressure of 9.6 kPa. When the target altitude was reached, the air intake rate was maintained at 15 L/min, together with the air extraction rate at 20 L/min, oxygen concentration at 20%, humidity at 60%, and temperature at 25°C. Rats in the NC and EE groups remained at 500 m altitude. At the end of the modeling, the condition of 6000 m altitude changed to normal altitude within 10 min. Finally, rats were removed from the chambers.

Rats were randomly assigned to 4 groups in the second part (seven animals in each group): NC group, HHM group, 3-MA group, and HHM + 3-MA group. 3-MA, an inhibitor of autophagosome formation, was dissolved in a solvent consisting of double-distilled water (ddH_2O), polyethylene glycol 300 (PEG300), dimethyl sulfoxide (DMSO), and Tween 80. It was intraperitoneally injected 1 hour prior to the hypobaric hypoxia exposure at a dose of 15 mg/kg. The other treatments were performed similarly to the first part of the research. The choice of 3-MA doses was based on a previously published study.[27] After being removed from the chambers, all rats were euthanized with an injection of sodium pentobarbital intraperitoneally.

In the third part, rats were randomly assigned to 4 groups (seven animals in each group): HHM group, EE100 group, HHM + RSL3 group, and EE 100 + RSL3 group. RSL3, a ferroptosis agonist, was dissolved in a solvent consisting of ddH2O, PEG300, DMSO, and Tween 80. It was intraperitoneally injected 1 hour prior to the hypobaric hypoxia exposure at a dose of 10 mg/kg. The other treatments were performed similarly to the first part of the research. The choice of RSL3 doses was based on a previously published study.[28]

The fourth part of the research aimed at verifying the mechanism of Keap1-Nrf2 axis in regulating ferritinophagy-mediated ferroptosis. Rats were randomly divided into four groups of seven rats each: HHM group, EE100 group, HHM + ML385 group, and EE 100 + ML385 group. For the ML385 groups, rats were injected intraperitoneally with ML385, a specific inhibitor of Nrf2 dissolved in a solvent consisting of Tween 80, PEG, ddH2O, and DMSO. ML385 was administrated 1 hour prior to the hypobaric hypoxia exposure at a dose of 30 mg/kg. The dosage and route of administration of ML385 were determined based on a previously published study.[29] The other groups received treatments similar to the first part of the research. After being removed from the chambers, all rats were euthanized with an injection of sodium pentobarbital. The route of sodium pentobarbital (50mg/Kg) administration for anesthesia and sacrifice was intraperitoneal injection.

Arterial Blood Gas Analysis

Rats were intraperitoneally anesthetized with pentobarbital sodium and the blood was collected from the abdominal aorta using negative pressure tubes containing lithium heparin. Approximately 0.1 mL of arterial blood was collected in samples and analyzed with a blood gas analyzer (Siemens EPOC, Ottawa, Canada). The obtained values included pH, partial pressure of carbon dioxide ($PaCO_2$), partial pressure of oxygen (PaO_2), arterial oxygen saturation (SaO_2), bicarbonate (HCO_3), hemoglobin (Hb), and hematocrit (Hct).

Lung Wet/Dry (W/D) Weight Ratio

We measured the lung W/D weight ratio to assess the severity of edema.[30] After 48 hours of hypobaric and hypoxia exposure, the wet weight of the left superior lobe was determined with an electronic balance (precision of 0.1 mg). The dry weight was determined after oven-drying of lung tissues at 60°C for 48 hours.

Histopathology

Part of the right lower lung lobe was rapidly removed, rinsed with PBS buffer, and fixed in 4% paraformaldehyde (at 4°C for 12 hours). Consecutively, the tissues were embedded in paraffin wax and sectioned into 4-micron slices, followed by hematoxylin and eosin (H&E) staining. The histopathological changes in the lung and bronchi were observed using optical microscopy (model: BX41, manufactured by Olympus Corporation, Tokyo, Japan). Lung injury scoring was performed in a blinded fashion by two pathologists using a semi-quantitative method. Lung injury was semiquantitatively assessed based on the following morphological criteria: alveolar septae, alveolar hemorrhage, intra-alveolar fibrin, and intra-alveolar infiltrates. Each parameter was scored on a scale of 0 to 3, as previously described.[31] The total lung injury score was calculated as the sum of the scores for all parameters.

TNF-α, VEGF, IL-6, and Total Protein Levels in BALF

After sacrifice, a ligation on the right lung of the rat was conducted with a hemostatic clamp. The left lung was gently washed two times with 0.5 mL of ice-cold phosphate buffered saline (PBS) to obtain the bronchoalveolar lavage fluid (BALF). BALF samples were centrifuged at 3000 ×g for 10 min at 4°C to remove the cell debris and the supernatant was stored immediately at −80°C until analysis. Levels of IL-6, VEGF, and TNF-α in the supernatant were detected using ELISA kits. The BCA protein assay kit was used to measure the total protein concentration in BALF.

Iron, MDA, GSH, and 4-HNE in Lung Tissues

A portion of the right lung was excised and washed to remove superficial blood. After homogenization with PBS, lung tissues were centrifuged, and the supernatants were removed. Measurement of iron, MDA, GSH, and 4-HNE in homogenates was performed using assay kits.

Measurement of Intracellular ROS Levels

Sterilized scissors and scalpels were used to cut the lung tissues into 3 to 5-mm-diameter pieces. Then, the lung tissue samples were cultured in PBS containing 0.2% collagenase type 2. The cell suspensions were filtered through a 200-mesh net to remove tissue fragments and cell clumps. Cell suspensions were centrifuged at 300 ×g for 5 min at 4°C and the supernatant was discarded. Subsequently, the cells were washed twice in PBS by centrifugation (5 minutes, 300 ×g, room temperature). Cells were resuspended in flow buffer, collected, and suspended in diluted dichlorodihydrofluorescein diacetate at a cell concentration of 1×10^6/mL. Then, cells were incubated in a tissue culture incubator (5% CO2, 37°C, 20 min). At last, cells were harvested and analyzed in a flow cytometer after being washed three times with a serum-free cell culture medium.

Transmission Electron Microscopy (TEM)

The lung tissues were fixed with 3% glutaraldehyde and the post-fixation was done with 1% osmium tetroxide. Dehydration of samples was achieved with concentration gradient acetone followed by embedding in EPON 812

resin. The resin blocks were ultra-thin sectioned at 60–90 nm with an ultramicrotome and mounted on copper grids. Staining of ultra-thin sections was conducted at room temperature for 15 min with uranyl acetate, followed by 2 min with lead citrate. Transmission electron microscopy (TEM) images were captured by JEM-1400Flash (Tokyo, Japan).

Immunofluorescence Staining

The paraffin-embedded lung tissues were sectioned to 4 μm thickness and were deparaffinized with xylene, and then rehydrated through a graded ethanol series. Antigen retrieval was conducted by boiling the fixed tissue sections in a 0.01 M sodium citrate buffer (pH 6.0) for 30 min. Then, the sections were cooled before washing 3 times with PBS for 5 min each. Later, tissue sections were blocked with 10% goat serum. Consecutively, the sections were incubated with the following antibodies overnight at 4 °C:anti-Nrf2 (1:100), and anti-GPX4 (1:100). The following day, the sections were incubated with biotinylated goat anti-rabbit immunoglobulins for one hour at room temperature. Finally, the sections were counterstained with 4'-6-diamidino-2-phenylindole (DAPI) to highlight the nuclei, and images were taken with a fluorescence microscope (Olympus, Tokyo, Japan). Fluorescence intensity was quantified using Image-J software.

Western Blotting

Following the sacrifice of rats, lung tissue samples were collected and snap-frozen in liquid nitrogen immediately. Then, lung tissue samples were preserved in a −80°C freezer. To prepare lysates, lung tissues were homogenized with a lysis buffer. Supernatants were collected after centrifugation of lung homogenates at 12000g.

Supernatant protein concentration was measured using a BCA assay kit. Proteins were separated by sodium dodecyl sulphate-polyacrylamide gel electrophoresis (SDS-PAGE). After electrophoresis, proteins were transferred onto polyvinylidene difluoride (PVDF) membranes. The membranes were then blocked with 5% non-fat milk or bovine serum albumin (BSA) in tris-buffered saline (TBS) containing 0.10% Tween 20 for 1 hour at room temperature. The membranes were incubated overnight at 4°C with the primary antibodies. On the second day, the PVDF membranes were incubated with horseradish peroxidase-conjugated secondary antibodies at room temperature for 2 hours. Detection of the protein bands was performed with enhanced chemiluminescence substrate and images were acquired with an image analyzer (Bio-Rad, USA).

Statistical Analysis

Data are expressed as mean ± standard error of the mean (SEM). Data with a normal distribution were evaluated by one-way analysis of variance (ANOVA). The Kruskal–Wallis test was performed when the data did not conform to a normal distribution. All statistical analyses were performed using GraphPad Prism 8.0 software (San Diego, CA, USA). A p-value < 0.05 was set as statistically significant.

Results

Eleutheroside E Effectively Mitigated the Severity of Lung Edema Induced by Hypobaric Hypoxia

We assessed pulmonary edema severity by measuring the lung W/D weight ratio. As depicted in Figure 1A, exposure to a hypobaric hypoxia environment significantly increased the W/D ratio in the HHM group. Notably, eleutheroside E pretreatment reversed the elevation in lung W/D weight ratio in a dose-dependent manner. Hypobaric hypoxia exposure led to an extensive amount of hemorrhage in the alveoli along with thickening of the alveolar walls, inflammatory cell infiltration, and alveolar and interstitial edema (Figure 1B and C). Importantly, eleutheroside E pretreatment markedly ameliorated the aforementioned pathological changes, and the degree of improvement exhibited a positive correlation with the administered dose. The VEGF, IL-6, TNF-α, and total protein levels in BALF increased following exposure to hypobaric hypoxia, indicating a large inflammatory exudation of the alveoli and bronchi. However, these elevations were reversed by eleutheroside E pretreatment. Eleutheroside E, akin to the positive control drug dexamethasone, counteracted the hypobaric hypoxia-induced rise in VEGF, IL-6, TNF-α and total protein in BALF, indirectly suggesting that eleutheroside E has a protective effect on HAPE (Figure 1D).

https://doi.org/10.2147/JIR.S577574

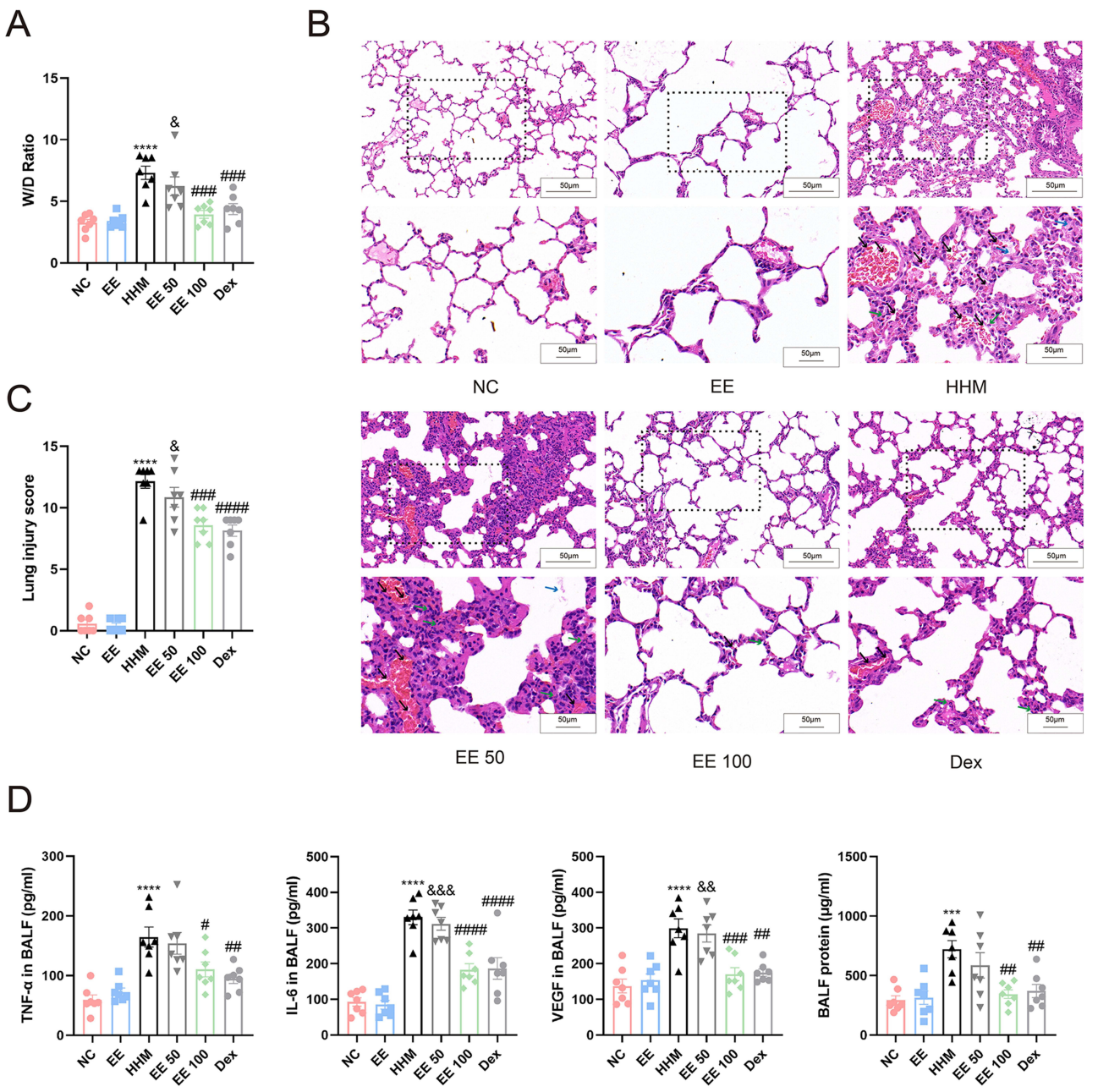

Figure 1 Eleutheroside E pretreatment attenuated lung edema. (**A**) Eleutheroside E improved lung edema (seven rats in each group). (**B**) Lung tissue sections were stained with H&E for histopathologic analysis. (four rats in each group, original magnification 200×, 400×, respectively). Black arrow: alveolar congestion, green arrow: infiltration of inflammatory cells; blue arrow: exudates in the alveolar space; (**C**) Histologic score of lung sections. (**D**) Effect of eleutheroside E on TNF-α, IL-6, VEGF, and total protein in BALF (seven rats in each group). ***P < 0.001, ****P<0.0001 vs. NC group; $^{\#}P$ < 0.05, $^{\#\#}P$ < 0.01, $^{\#\#\#}P$ <0.001, $^{\#\#\#\#}P$ <0.0001 vs. HHM group; $^{\&}P$ < 0.05, $^{\&\&}P$ < 0.01, $^{\&\&\&}P$ < 0.001 vs. EE 100 group. Data are expressed as mean ± SEM and analyzed by ANOVA.

Eleutheroside E Pretreatment Has Taken a Major Role in the Correction of Hypoxia in HAPE

In contrast to the NC group, the pH value was up-regulated in the HHM group, indicating that hypobaric hypoxia exposure led to disruptions in the acid-base balance. While the pH value exhibited a slight decrease in the EE50 and EE100 groups, these changes were not statistically significant. Following hypobaric hypoxia exposure, there were increases in PaCO2 and HCO3 concentrations, possibly due to hyperventilation. Although not statistically significant, pretreatment with eleutheroside E reversed the changes in $PaCO_2$ and HCO_3 concentration. At the same time, hypobaric

https://doi.org/10.2147/JIR.S577574

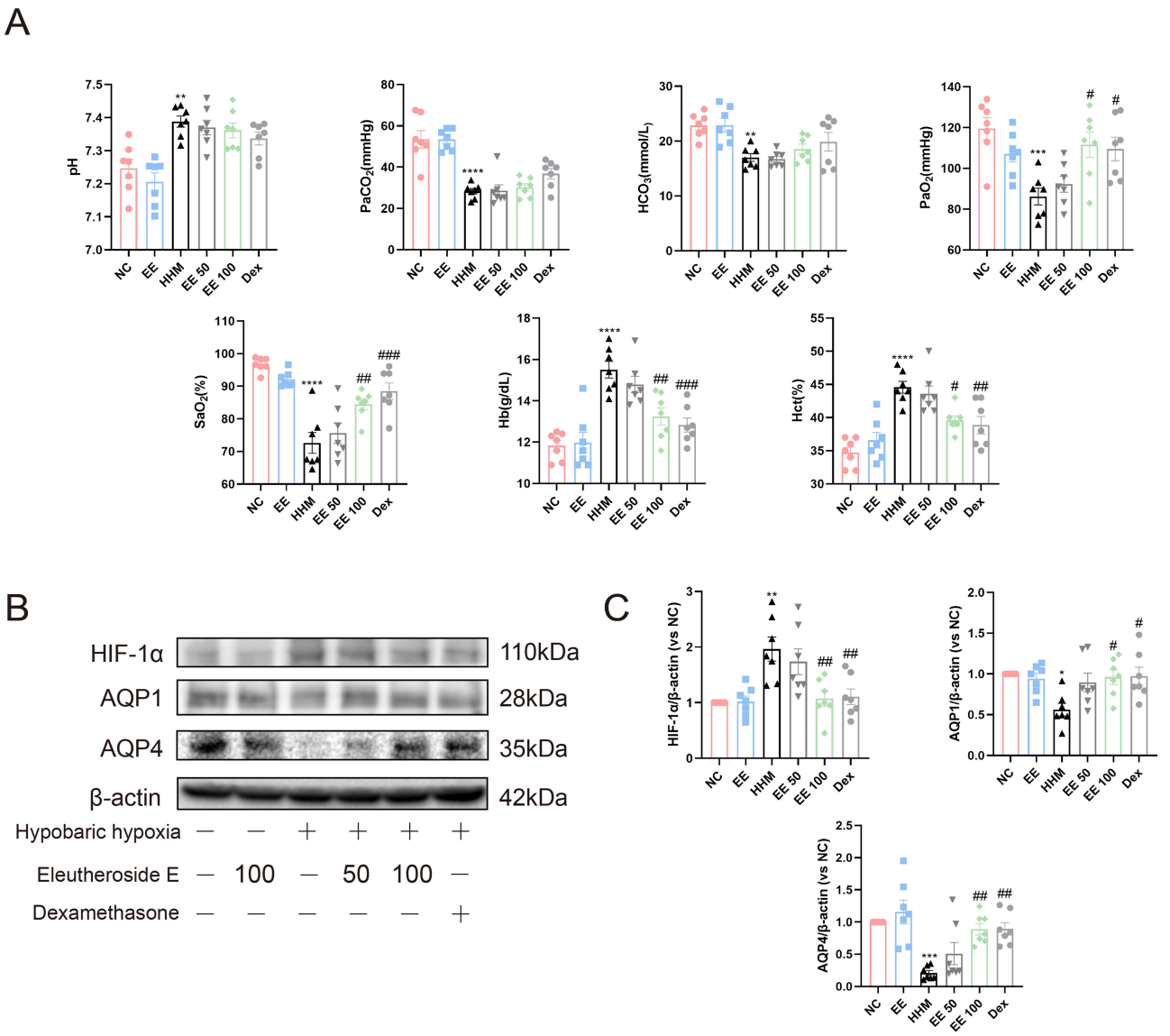

Figure 2 The effects of eleutheroside E in the correction of hypoxia in HAPE. **(A)** Effect of eleutheroside E on levels of pH, PaCO2, HCO3, PaO2, SaO2, Hb and Hct (seven rats in each group). (**B** and **C)** Proteins expression of HIF-1α, AQP1, and AQP4 (seven rats in each group). $^{**}P < 0.01$, $^{***}P < 0.001$, $^{****}P<0.0001$ vs. NC group; $^{\#}P < 0.05$, $^{\#\#}P < 0.01$, $^{\#\#\#}P <0.001$ vs. HHM group. Data are expressed as mean ± SEM and analyzed by ANOVA.

hypoxia exposure resulted in reduced PaO2 and SaO2 levels, but eleutheroside E pretreatment dose-dependently increased both PaO2 and SaO2. Additionally, Hb and Hct concentrations increased after hypobaric hypoxia exposure, whereas eleutheroside E pretreatment reversed the changes in Hb and Hct concentrations to some extent (Figure 2A).

As illustrated in Figure 2B and C, a significant up-regulation of hypoxia-inducible factor-1α (HIF-1α) and a significant inhibition of aquaporin 1 (AQP1) and aquaporin 4 (AQP4) were reported after hypobaric hypoxia exposure. Importantly, eleutheroside E pretreatment markedly reversed the aforementioned changes. These findings indicated that eleutheroside E holds promise as a potential therapeutic agent against HAPE.

Eleutheroside E Demonstrated Protective Effects in the Context of HAPE Through Its Anti-Oxidative Stress Properties

We observed that hypobaric hypoxia exposure induced an accumulation of ROS, whereas the ROS expression was suppressed by eleutheroside E pretreatment (Figure 3A). Furthermore, eleutheroside E exhibited a dose-dependent

https://doi.org/10.2147/JIR.S577574

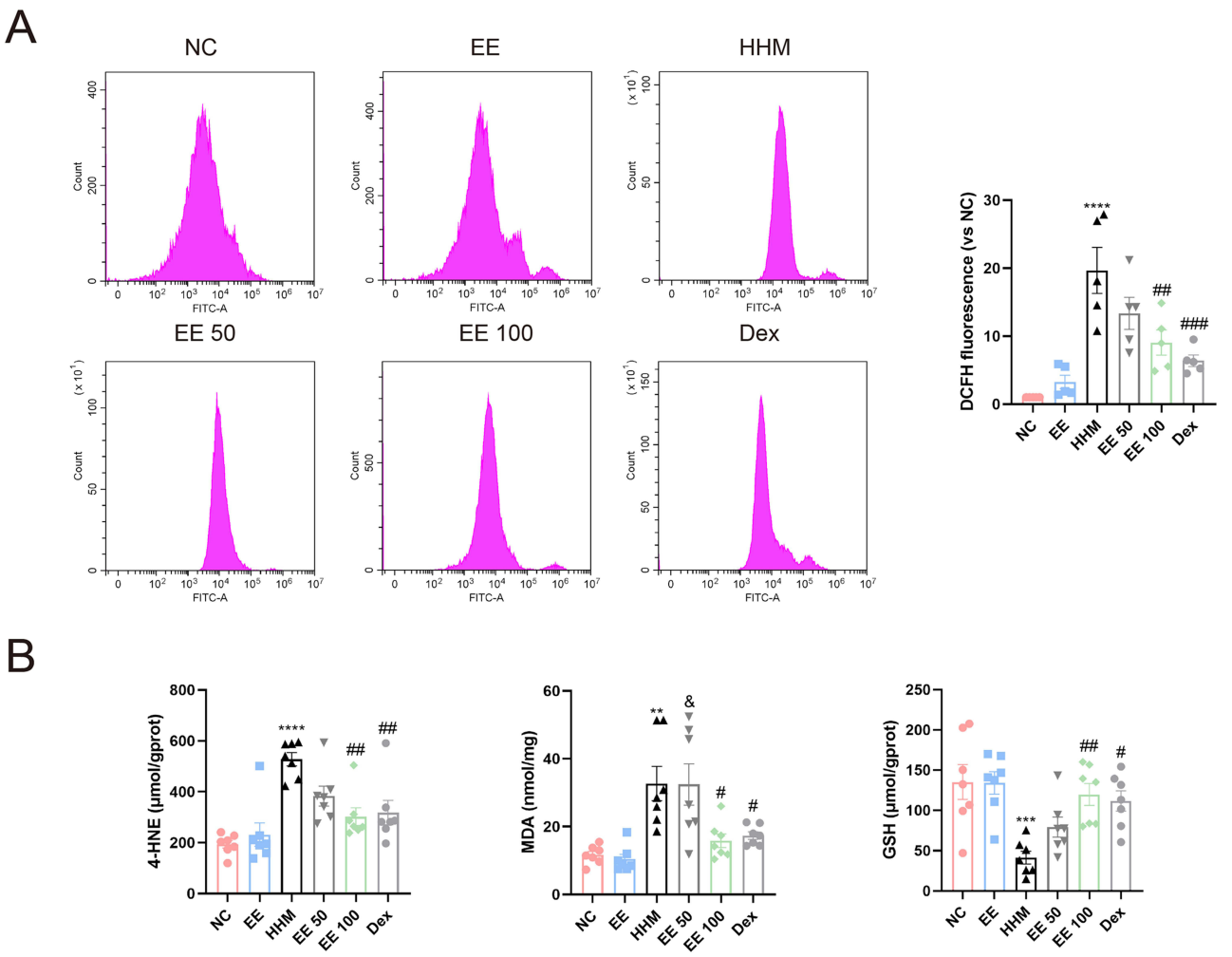

Figure 3 The anti-oxidant effects of eleutheroside E pretreatment in HAPE. (**A**) Effect of eleutheroside E on intracellular ROS levels (four rats in each group). (**B**) Effect of eleutheroside E on 4-HNE, MDA, and GSH (seven rats in each group). $^{**}P < 0.01$, $^{***}P < 0.001$, $^{****}P<0.0001$ vs. NC group; $^{\#}P < 0.05$, $^{\#\#}P < 0.01$, $^{\#\#\#\#}P <0.001$ vs. HHM group; $^{\&}P < 0.05$ vs. EE 100 group. Data are expressed as mean ± SEM and analyzed by ANOVA.

capacity to reverse the alterations in 4-HNE, MDA, and GSH triggered by hypobaric hypoxia (Figure 3B). These above findings underscored that hypobaric hypoxia exposure resulted in oxidative stress, excessive ROS production, and a disruption of the redox balance. Notably, eleutheroside E pretreatment successfully counteracted these aforementioned changes.

Eleutheroside E Exerts a Negative Regulatory Effect on Ferritinophagy in HAPE

Ferritinophagy is governed by the cargo receptor NCOA4, which directly interacts with FTH1, leading to the delivery of the ferritin complex to autophagosomes for lysosomal degradation and iron release.[32] Under electron microscopy, it was evident that autolysosomes accumulated, and typical morphological changes associated with ferroptosis were observed in the HHM group compared to the NC group. However, treatment with eleutheroside E effectively reduced the accumulation of autolysosomes and reversed the mitochondrial morphological changes associated with ferroptosis. This implies that eleutheroside E, in part, functions by inhibiting ferritinophagy. (Figure 4A). Subsequently, the iron content in the tissues was measured. In the HHM group, overactivated autophagy led to the degradation of ferritin and the release of free iron ions. Notably, eleutheroside E application reduced this iron release, indirectly indicating its protective effect against HAPE (Figure 4B). For further validation, markers of ferritinophagy, including SQSTM1, FTH1, NCOA4, and TFRC, were examined using Western blotting. The detected bands are presented in Figure 4C and D. The protein

 https://doi.org/10.2147/JIR.S577574

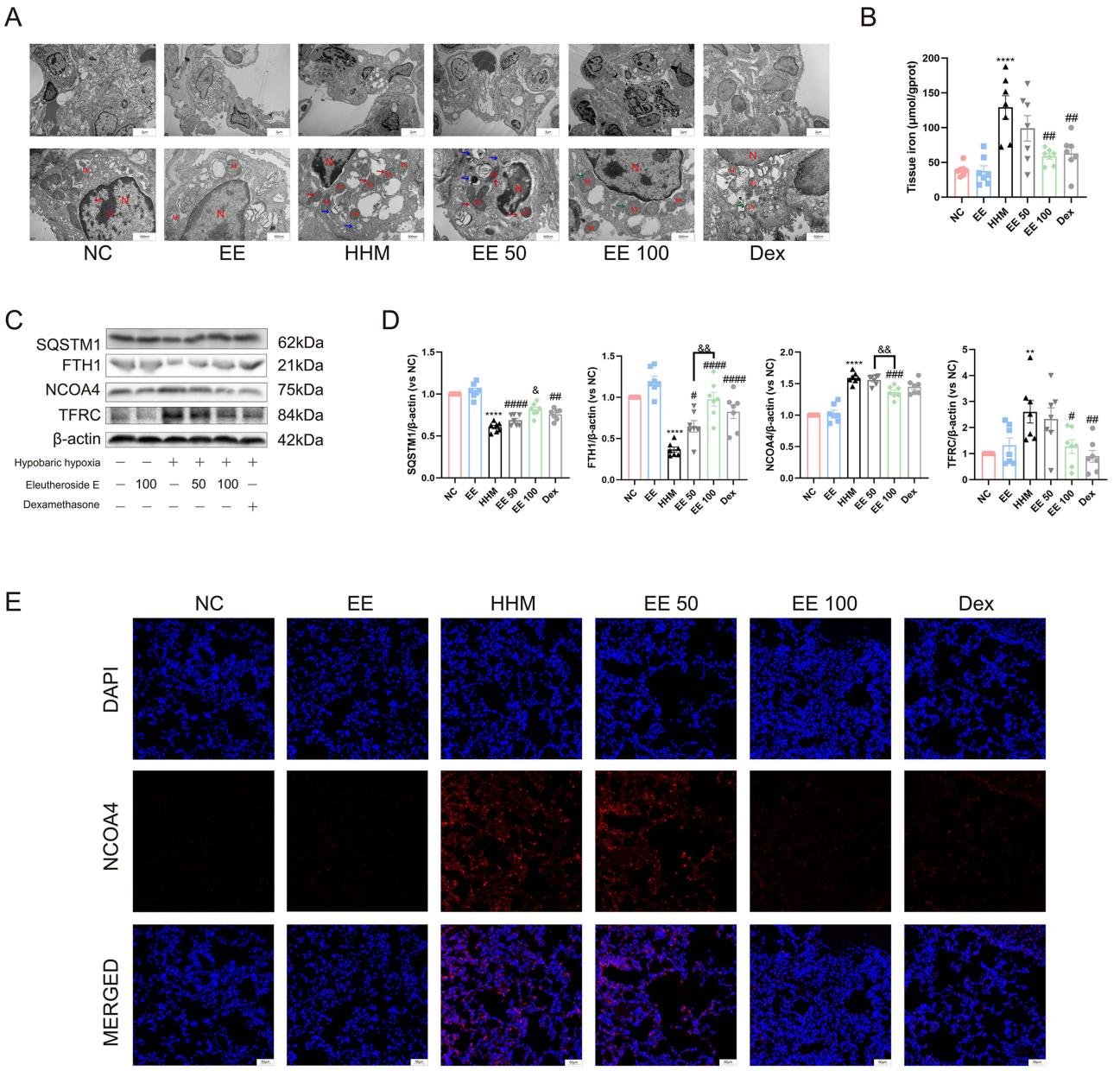

Figure 4 Eleutheroside E suppress ferritinophagy in HAPE. (**A**) The remarkable images of ferritinophagy ultrastructure by TEM (four rats in each group, original magnification 6000×, 25,000×, respectively). Red arrows: mitochondrial changes of ferroptosis; blue arrows: autolysosomes. (**B**) Eleutheroside E suppressed iron release in lung tissue (seven rats in each group). (**C** and **D**) Proteins expression of SQSTM1, FTH1, NCOA4, and TFRC (seven rats in each group). (**E**) Immunofluorescence assays of NCOA4. (four rats in each group, original magnification 200×). $^{**}P < 0.01$, $^{****}P<0.0001$ vs. NC group; $^{\#}P < 0.05$, $^{\#\#}P < 0.01$, $^{\#\#\#\#}P <0.001$, $^{\#\#\#\#\#}P <0.0001$ vs. HHM group; $^{\&}P < 0.05$, $^{\&\&}P < 0.01$ vs. EE 100 group. Data are expressed as mean ± SEM and analyzed by ANOVA.

expression levels of SQSTM1 and FTH1 were significantly lower in the HHM group and higher in the EE groups, with a dose-dependent relationship. Furthermore, NCOA4 and TFRC expression were significantly increased in the HHM group but decreased in the EE100 group. We also verified the expression of NCOA4, a ferritinophagy-related protein, through immunofluorescence staining. Immunofluorescence staining of lung tissues showed that NCOA4 expression was enhanced by hypobaric hypoxia exposure, and eleutheroside E administration markedly reversed these changes (Figure 4E). Taken together, eleutheroside E effectively inhibits the expression of ferritinophagy-related proteins in hypoxic lung tissues, and this inhibition is positively correlated with the dosage of eleutheroside E. This suggests that eleutheroside E mitigates autophagy, thus suppressing iron release in lung tissues exposed to a hypobaric hypoxic environment.

https://doi.org/10.2147/JIR.S577574

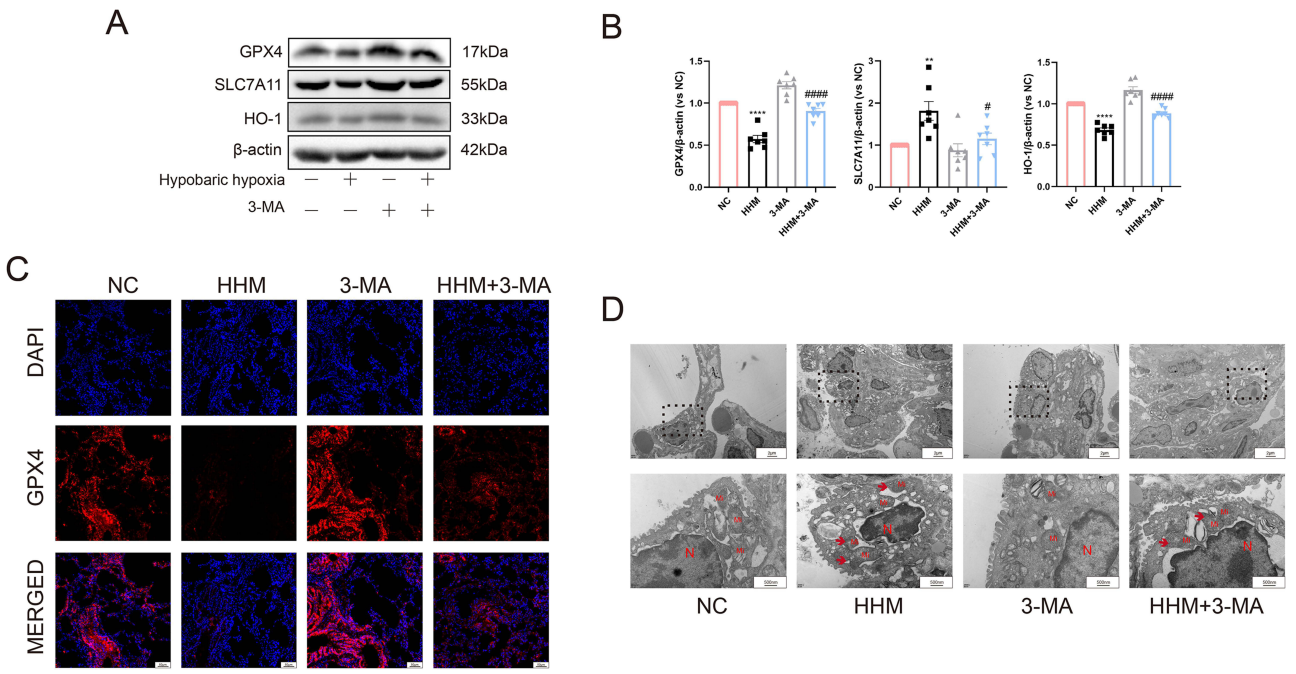

Figure 5 Autophagy facilitated ferroptosis in HAPE. (**A** and **B**) Proteins expression of GPX4, SLC7A11, and TFRC (seven rats in each group). (**C**) Immunofluorescence assays of GPX4. (four rats in each group, original magnification 200×). (**D**) The remarkable images of ferroptosis ultrastructure by TEM (four rats in each group, original magnification 6000×, 25,000×, respectively). Red arrows: mitochondrial changes of ferroptosis. *****P*<0.0001 vs. NC group; #*P* < 0.05, ####*P* <0.0001 vs. HHM group. Data are expressed as mean ± SEM and analyzed by ANOVA.

Inhibition of Autophagy Diminished Hypobaric Hypoxia-Induced Ferroptosis

We employed 3-MA, an early-stage autophagy inhibitor, to hinder the formation of autophagosomes and investigated its impact on ferroptosis. Associated proteins were detected by immunoblot to verify the impact of autophagy on ferroptosis. As depicted in Figure 5A and B, lung GPX4, SLC7A11, and HO-1 expression decreased after exposure to hypobaric hypoxia. However, 3-MA administration significantly improved the protein expression levels of these ferroptosis markers. It can be inferred that the inhibition of autophagy may alleviate ferroptosis-induced tissue injury. Through immunofluorescence staining, we found that GPX4 protein expression was elevated compared with that of the HHM group following the administration of 3-MA (Figure 5C). Moreover, electron microscopic analysis of alveolar type II epithelial cells shows reduced mitochondrial volume, increased mitochondrial electron and membrane densities, and decreased mitochondrial cristae junctions. These changes in mitochondrial morphology are characteristic features of ferroptosis. Significantly, treatment with 3-MA, an autophagy inhibitor, reduced this form of cell death (Figure 5D). Thus, the role of autophagy on ferroptosis was investigated in the current study, highlighting that autophagy may facilitate ferroptosis through a specific form of cargo-specific autophagy known as ferritinophagy.

RSL3 Application Weakened the Inhibitory Effects of Eleutheroside E on Ferritinophagy

Our findings demonstrate that ferritinophagy, a novel form of autophagy, promotes ferroptotic cell death in HAPE; and eleutheroside E alleviates autophagy to suppress ferroptosis under a hypobaric hypoxic environment. In further validation, RSL3, a specific agonist, was applied to verify the impact of ferroptosis on ferritinophagy. Compared with the EE100 group, we observed contrasting trends in the expression of SQSTM1, FTH1, NCOA4, and TFRC in rats treated with RSL3 (Figure 6A and B). This suggests that the occurrence of ferroptosis has some degree of influence on ferritinophagy. We investigated the ultrastructural changes of lung tissue under an electron microscope, and typical features of mitochondrial morphology associated with ferroptosis were evident. Compared to the EE100 group, RSL3 treatment increased the number of autolysosomes and enhanced mitochondrial morphological changes indicative of

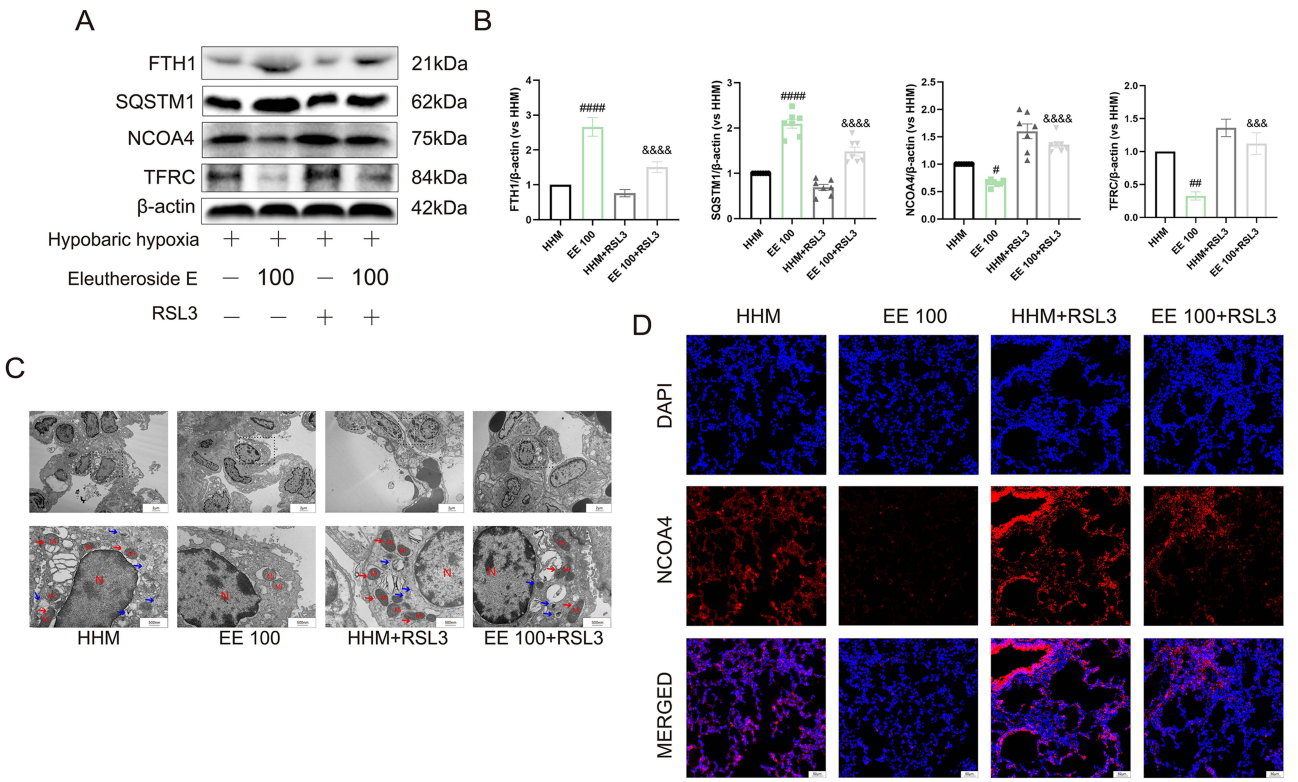

Figure 6 Effects of ferroptosis activation on ferritinophagy in eleutheroside E against HAPE. (**A** and **B**) Proteins expression of FTH1, SQSTM1, NCOA4, and TFRC (seven rats in each group). (**C**) The remarkable images of ferritinophagy ultrastructure by TEM (four rats in each group, original magnification 6000×, 25,000×, respectively). Red arrows: mitochondrial changes of ferroptosis; blue arrows: autolysosomes. (**D**) Immunofluorescence assays of NCOA4 (four rats in each group, original magnification 200×). $^{\#}P < 0.05$, $^{\#\#}P < 0.01$, $^{\#\#\#\#}P < 0.0001$ vs. HHM group; $^{\&\&\&}P < 0.001$, $^{\&\&\&\&}P < 0.0001$ vs. EE 100 group. Data are expressed as mean ± SEM and analyzed by ANOVA.

ferroptosis (Figure 6C). Through immunofluorescence staining, we found that NCOA4 protein expression was elevated in comparison to the EE100 group following the administration of RSL3 (Figure 6D). Our earlier confirmation indicated that eleutheroside E pretreatment ameliorated ferrintinophagy against HAPE, while the anti-ferrintinophagy effects of eleutheroside E were diminished by RSL3 application. The results indirectly elucidated that autophagy and ferroptosis are subject to complex reciprocal regulation in HAPE.

Eleutheroside E Alleviated Ferritinophagy-Mediated Ferroptosis in HAPE via the Keap1-Nrf2 Axis

We have previously established that ferroptosis is intricately involved in the development of HAPE and that eleutheroside E exerts a negative regulatory effect on ferritinophagy in this context. To investigate the regulatory effect of eleutheroside E on ferroptosis-related proteins, including GPX4 and SLC7A11, we conducted Western blot assays. As indicated in Figure 7A and B, eleutheroside E elevated the levels of GPX4 and SLC7A11 in a dose-dependent manner, with the highest dose of eleutheroside E showing the most significant effect. Nrf2 is negatively regulated by the Keap1 protein, which plays a crucial role in mediating the ferritinophagy-dependent activation of ferroptosis.[33] Our results suggested that the hypobaric hypoxia exposure up-regulated Keap1 expression and down-regulated Nrf2 expression compared to the NC group. However, eleutheroside E treatment partially reversed these trends (Figure 7A and B).

In the following section, we employed ML385, an Nrf2 inhibitor, to validate the influence of the Keap1-Nrf2 axis in ferritinophagy-mediated ferroptosis. In contrast to the EE100 group, Keap1 protein expression decreased, and Nrf2 protein expression increased after ML385 application (EE100 + ML385 group), thereby contributing to the alterations in ferritinophagy-related proteins. The trends observed in the bands of SQSTM1, FTH1, NCOA4, TFRC, and GPX4, which were modulated by eleutheroside E, were reversed after ML385 treatment (Figure 8A and B). Immunofluorescence double staining of Nrf2 and NCOA4 was performed to demonstrate changes in ferritinophagy-associated proteins. In

https://doi.org/10.2147/JIR.S577574

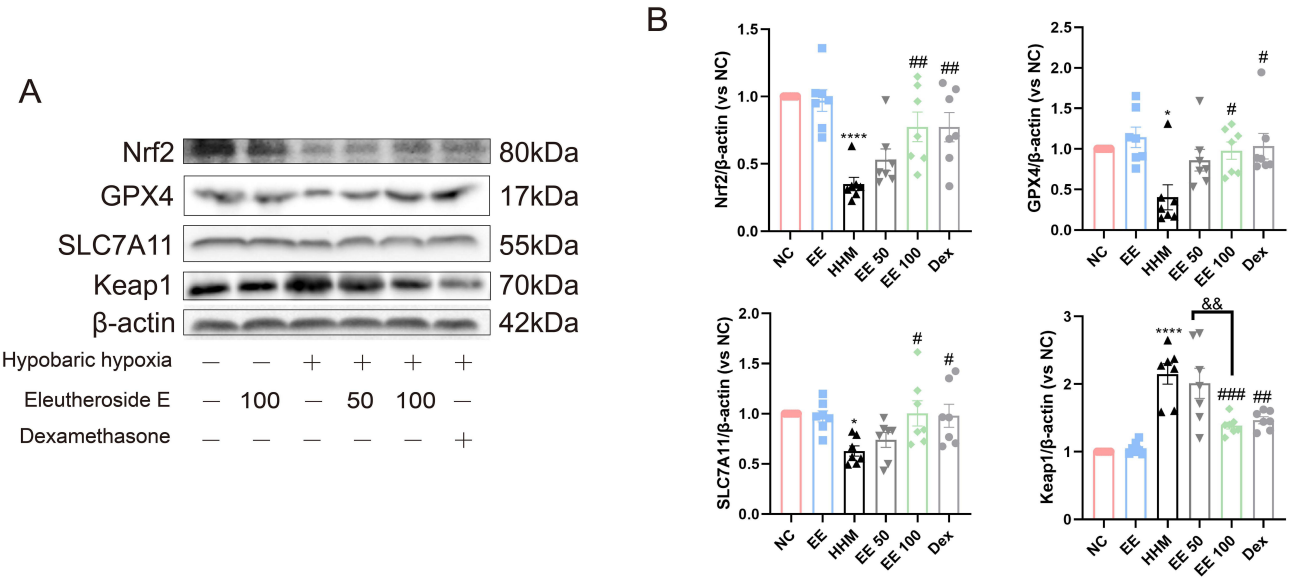

Figure 7 The effect of eleutheroside E on ferritinophagy-mediated ferroptosis. (**A** and **B**) Proteins expression of Nrf2, GPX4, SLC7A11, and Keap1 (seven rats in each group). *P<0.05, ****P<0.0001 vs. NC group; $^{\#}P$ < 0.05, $^{\#\#}P$ < 0.01, $^{\#\#\#\#}P$ < 0.001 vs. HHM group; $^{\&\&}P$ < 0.01 vs. EE 100 group. Data are expressed as mean ± SEM and analyzed by ANOVA.

comparison to the HHM group, lung tissues exhibited enhanced Nrf2 fluorescence intensity and attenuated NCOA4 fluorescence intensity in the EE100 group, respectively. However, this trend was found to be reversed in the EE100 +ML385 group (Figure 8C). H&E staining showed that ML385 triggered inflammatory cell infiltration and alveolar hemorrhage in the EE100 + ML385 group compared to the EE100 group (Figure 8D). It appears that ML385 injection counteracted the anti-ferritinophagy effects of eleutheroside E. These findings reinforced that eleutheroside E might have a therapeutic role against HAPE by modulating ferritinophagy-mediated ferroptosis via the Keap1-Nrf2 axis.

Discussion

Our research uncovered that extreme plateau environments can trigger oxidative stress and ferritinophagy-mediated ferroptosis, ultimately contributing to pulmonary edema. The results indicated that eleutheroside E has therapeutic effects on high-altitude pulmonary edema. In addition, the anti-ferritinophagy molecular mechanisms of eleutheroside E against HAPE were validated through experiments in vivo (Figure 9).

HAPE is a condition characterized by an abnormal accumulation of fluids in the lungs, often occurring at altitudes exceeding 3000 meters.[34] Eleutheroside E has been shown to reduce ischemia-reperfusion (I/R) injury by inhibiting inflammation and intracellular ROS production.[35] Moreover, eleutheroside E showed therapeutic potential against edema through modulation of the endothelial barrier function and exhibited anti-fatigue effects via improvement of exercise tolerance in mice.[36,37] Given these findings, we explored whether eleutheroside E could be beneficial in an animal model of HAPE.

Hypoxia-stimulated inflammatory chemokines may contribute to the progression of HAPE by damaging lung endothelial cells.[38] In addition, hypoxia may increase the pulmonary capillary pressure and cause capillary leakage. Inflammatory mediators are soluble proteins actively secreted by resident and infiltrating immune cells into the airway lumen and alveolar space.[39] In the pathophysiological process of HAPE, the alveolar-capillary barrier represents the primary site of injury, where inflammatory cytokines act locally to modulate endothelial and epithelial permeability.[40] Cytokines measured in BALF reflect dynamic inflammatory responses with high sensitivity, as they represent the balance between local production and clearance within the alveolar space.[41] Key ferroptosis markers (eg., GPX4, SLC7A11, and ferritin) are intracellular proteins that require tissue lysis or histological sectioning for accurate quantification; these markers cannot be reliably detected in BALF because they are not actively secreted.[42] In our study, hypobaric hypoxia exposure significantly increased the total protein content in BALF. Large amounts of proteins can enter into the alveolar

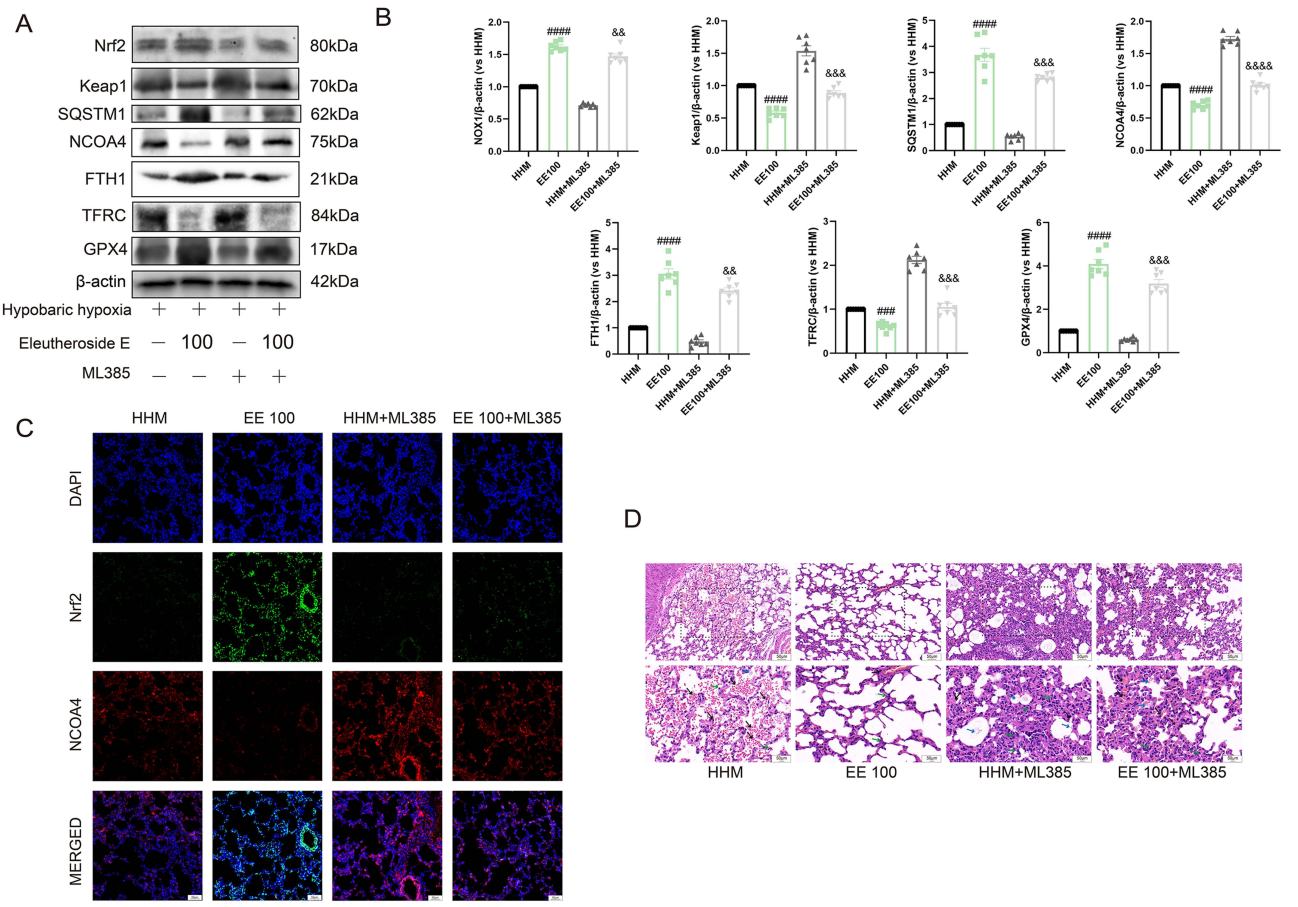

Figure 8 The inhibitory effect of eleutheroside E on ferritinophagy-mediated ferroptosis was abolished by ML385. (**A** and **B**) Proteins expression of Nrf2, Keap1, SQSTM1, NCOA4, FTH1, TFRC, and GPX4 (seven rats in each group). (**C**) Immunofluorescence assays of Nrf2 and NCOA4 (four rats in each group, original magnification 200×). (**D**) Lung tissue sections were stained with H&E for histopathologic analysis. (four rats in each group, original magnification 200×, 400×, respectively). Black arrow: alveolar congestion, green arrow: infiltration of inflammatory cells; blue arrow: exudates in the alveolar space. $^{\#\#\#\#}P < 0.001$, $^{\#\#\#\#\#}P < 0.0001$ vs. HHM group; $^{\&\&}P < 0.01$, $^{\&\&\&}P < 0.001$, $^{\&\&\&\&}P < 0.001$ vs. EE 100 group. Data are expressed as mean ± SEM and analyzed by ANOVA.

spaces and pulmonary tissues, resulting in lung edema. We have also identified high expression levels of VEGF in BALF. VEGF is a mediator playing a pivotal role in the development of pulmonary edema.[43] IL-6 is one of the major factors influencing the acute phase protein synthesis during the acute phase response.[44] TNF-α is involved in promoting neutrophil production and activation, thus causing inflammation and tissue injury.[45] Consistently with previously published studies,[46] we found that IL-6 and TNF-α levels in BALF markedly increased after hypobaric hypoxia exposure.

Low oxygen pressure and low oxygen content are characteristics of high altitudes, leading to inadequate tissue oxygenation,[47] The blood gas analysis indicated a high pH in the HHM group, possibly caused by obstruction of oxygen exchange in the alveoli of the lungs. The observed changes in pH induced by hypobaric hypoxia appeared not consistent with a previous study.[48] The differences might be due to different altitudes, different durations of hypobaric hypoxia exposure, and different ascent behaviors. PaO2 and PaCO2 were reduced by a hypobaric hypoxia exposure of 48 hours at 5000 m of altitude, possibly because the activation of carotid chemoreceptors resulted in hyperventilation and hypocapnia. In addition, hypoxia stress may increase hemoglobin and hematocrit levels. Elevated hemoglobin levels increase the oxygen-carrying capacity of blood, compensating for hypoxic hypoxia at high altitudes.[49] We showed similar findings in our hypobaric hypoxia group.

HIF-1α is a well-known biomarker for hypoxia. It is involved in the hypoxia-mediated effects of TNF-α.[50] The effects of eleutheroside E may reduce TNF-α expression through inhibition of HIF-1α. An essential component of HAPE pathogenesis is the disruption of alveolar-capillary barrier integrity. Exposure to hypobaric hypoxia triggers uneven

https://doi.org/10.2147/JIR.S577574

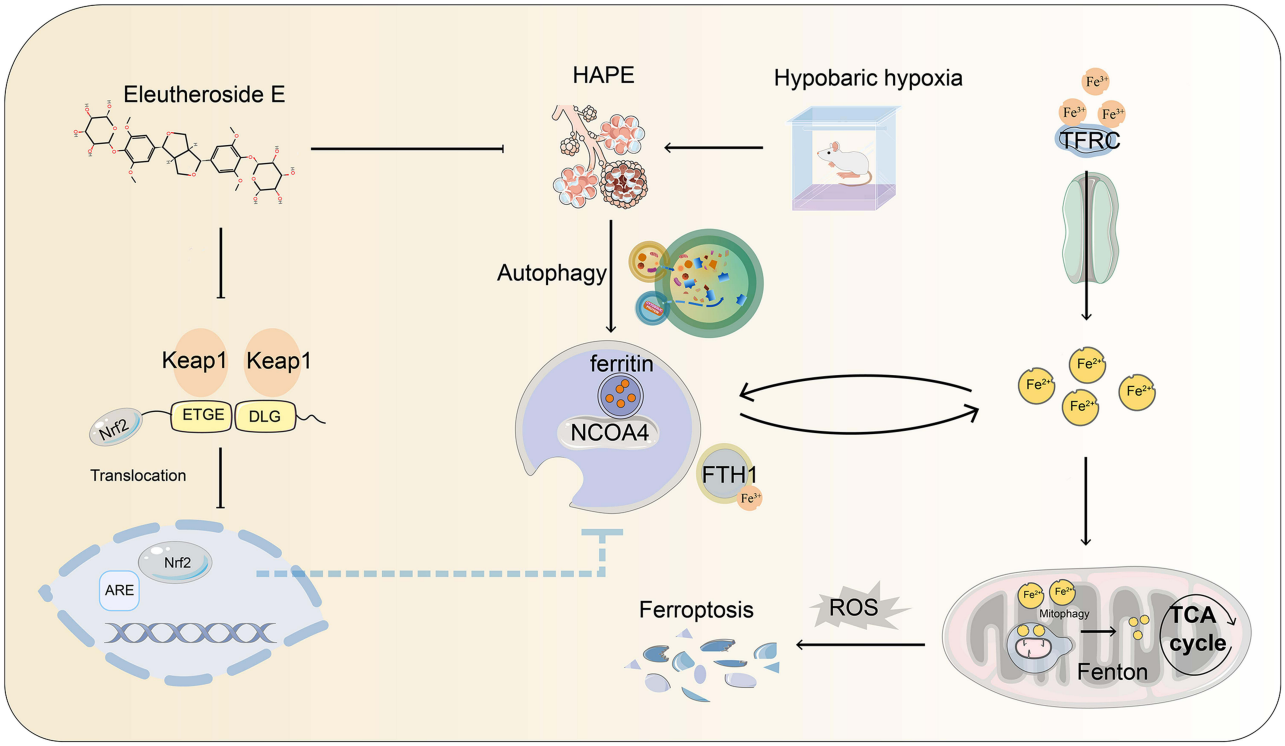

Figure 9 The protective effect of eleutheroside E on HAPE and the underlying mechanisms.

hypoxic pulmonary vasoconstriction, leading to "stress failure" of pulmonary capillaries and subsequent ultrastructural damage to endothelial and epithelial membranes, as confirmed by electron microscopic observations.[1,51] This barrier disruption increases vascular permeability and initiates local inflammatory responses, collectively compromising pulmonary fluid homeostasis. Aquaporins (AQPs), particularly AQP1 and AQP4, are water channel proteins crucial for maintaining lung fluid balance. AQP1 is primarily localized to pulmonary capillary endothelial cells, while AQP4 is expressed in alveolar epithelial cells. Under physiological conditions, these AQPs facilitate transcellular water movement and contribute to the active reabsorption of interstitial and alveolar fluid. However, when the alveolar-capillary barrier is compromised by hypoxic injury, the expression and membrane localization of AQP1 and AQP4 may become dysregulated.[52] Thus, the interplay between barrier disruption and AQP dysfunction represents a critical determinant of HAPE progression. A previous study found that the expression of aquaporin-1 was downregulated in a model of HAPE.[53] Similarly, an augmented expression of AQP4 was considered protective against lung edema.[54] Eleutheroside E was beneficial for HAPE through the modulation of HIF-1α, AQP1, and AQP4 expression levels.

A high-altitude hypoxic environment alters oxygen homeostasis and stimulates oxidative stress. Proteins, lipids, and nucleic acids can be easily oxidized in the presence of ROS, leading to irreversible damage to DNA, cell membranes, and other cellular structures.[55] 4-HNE, an unsaturated hydroxyalkenal, derives from lipid peroxidation and is used as a tissue marker for lipid peroxidation.[56] Membrane lipid peroxidation produces MDA, an enzyme damaging the mitochondrial respiration chain.[57] Contrary to 4-HNE and MDA, GSH counterbalances the effects of ROS and alleviates the damage of free radicals. We found that the expression of the aforementioned markers of oxidative stress was consistent with the ROS results.

Several pathways of programmed cell death are involved in high-altitude illness, including autophagy, senescence, and apoptosis.[58–60] Ferroptosis is characterized by significant elevation in intracellular labile iron level, ROS, and lipid peroxides, serving crucial roles in hypoxic diseases. Exposure to high altitude resulted in substantial and wide-ranging alterations in iron metabolism, resulting in iron overload, which can catalyze the production of free radicals through the Fenton reaction.[14] A recent study revealed that acute high-altitude hypoxia exposure triggered increasing brain

formaldehyde levels, contributing to neuronal ferroptosis.[12] Such ferroptosis-related mitochondria morphological changes were also observed in AECII with hypobaric hypoxia in our study. The inactivation of GPX4 and subsequent accumulation of ROS serve as central regulators of ferroptosis.[61] The link between ferroptosis and alveolar-capillary barrier dysfunction likely involves multiple interconnected mechanisms. First, ferroptotic cell death directly eliminates barrier-forming cells. Pulmonary endothelial cells and alveolar epithelial cells are both susceptible to ferroptosis under oxidative stress conditions, and their loss creates physical gaps that permit fluid and protein leakage.[62] Second, lipid peroxidation—the hallmark of ferroptosis—can disrupt intercellular junctions before overt cell death. 4-Hydroxynonenal (4-HNE), a major lipid peroxidation product, has been shown to covalently modify and destabilize VE-cadherin and ZO-1, compromising endothelial and epithelial barrier integrity.[63] Third, ferroptotic cells release damage-associated molecular patterns (DAMPs) including HMGB1, oxidized lipids, and cell-free DNA, which activate pattern recognition receptors on adjacent cells and infiltrating immune cells. This triggers a pro-inflammatory cascade (eg., IL-1β, TNF-α production) that further increases vascular permeability and recruits additional inflammatory cells, creating a vicious cycle.[64] Collectively, these mechanisms converge to disrupt alveolar-capillary barrier integrity and promote HAPE.

From another aspect, research on the correlation between autophagy and ferroptosis has become a hot topic. Ferritinophagy is a form of selective autophagy responsible for degrading intracellular ferritin, mediated by NCOA4. Given that NCOA4-mediated ferritinophagy directly liberates redox-active iron, we reason that ferritinophagy likely represents an upstream trigger. This is consistent with studies showing that ferritinophagy activation precedes ferroptosis in other cell types under oxidative stress conditions.[65] Once ferroptosis is initiated, the resulting accumulation of lipid peroxides and mitochondrial dysfunction may further promote iron dyshomeostasis, creating a positive feedback loop that amplifies ferritinophagy.[66] While our data reveal reciprocal regulation, the precise nature of this amplification mechanism requires future investigation using time-course analyses and sequential inhibition approaches. Electron microscopy in our current research has already revealed the autolysosome accumulation and typical morphological changes associated with ferroptosis under hypobaric hypoxia exposure. Our study unveiled that eleutheroside E alleviates autophagy, thereby suppressing iron release in lung tissues under hypobaric hypoxic conditions. SQSTM1 is an autophagy substrate, and the reduction of SQSTM1 serves as a marker of autophagy activation.[67] We demonstrated that eleutheroside E modulates the ferritinophagy-related proteins, including autophagy marker proteins (SQSTM1, NCOA4) and iron metabolism-related proteins (FTH1, TFRC). Clearly, the suppression of ferritinophagy-mediated ferroptosis could be a candidate mechanism underlying the therapeutic action of eleutheroside E against HAPE.

Regarding to the role of autophagy in HAPE-associated ferroptosis, we demonstrated that autophagy regulates ferroptosis by using 3-MA, an autophagy inhibitor. Conversely, we also applied RSL3 in our research to confirm the modulation of ferroptosis on ferritinophagy. Through a combination of several experimental approaches, including immunoblotting, electron microscopy, and immunoelectron microscopy, accumulating evidence strongly indicates the involvement of autophagy and ferroptosis in the pathological process of HAPE. Ferritin can be degraded by autophagy with the assistance of NCOA4, which drives ferritin to the lysosome and subsequent iron release, contributing to the release of free iron and resulting in ferroptosis. However, the current study primarily focused on ferritinophagy-mediated ferroptosis in HAPE. Other types of autophagy, such as lipophagy, clockophagy, and chaperone-mediated autophagy, may also contribute to the induction of ferroptosis by degrading negative regulators of ferroptosis.[68,69] Further investigation is needed to understand the specific molecular mechanisms of ferritinophagy, the role of other autophagy types in ferroptosis regulation, and the interactions and feedback loops between autophagy and ferroptosis in HAPE.

Previous studies indicated that Nrf2 activation could be a potential candidate for high-altitude illness prevention.[7,70] Research showed that the Keap1-Nrf2 axis may also be involved in autophagy and ferroptosis regulation.[71,72] Nrf2 facilitates the ubiquitylation and degradation of NCOA4 by the proteasome, leading to the inhibition of ferritinophagy and a reduction in cell sensitivity to ferroptosis.[73] However, Nrf2 also directly impacts autophagy, and knocking down Nrf2 resulted in an increase in autophagy.[74] Keap1, a negative regulator of Nrf2, directly mediates the ubiquitylation and proteasomal degradation of Nrf2, involving in regulation of oxidative stress and ferritinophagy. Our experiments suggested that eleutheroside E exerted therapeutic effects on HAPE by suppressing ferritinophagy-mediated ferroptosis via the Keap1-Nrf2 axis. GPX4, as well as HO-1 and SLC7A11 are downstream genes of the Keap1-Nrf2 axis that reduce ROS levels and ferroptosis.[75–77] FTH1 is responsible for the oxidation of Fe^{2+} to Fe^{3+}, impeding the oxidative

damage possibly caused by Fenton reactions.[78] TFRC, along with FTH1, NCOA4, and SQSTM1, were identified as critical ferritinophagy proteins. The changes in the aforementioned ferritinophagy-related proteins were in accordance with our findings. Only a few studies reported different Nrf2 behaviors in hypoxia models.[8,79] The discrepancy may be explained by different altitudes, different durations of hypobaric hypoxia exposure, and variability across animals and tissues. It is possible that Keap1 dissociates from Nrf2, allowing Nrf2 to translocate into the nucleus in an attempt to compensate for the early stages of HAPE. However, when oxidative stress becomes too high, the effect of Nrf2 dissociation from Keap1 may not be sufficient to counteract the oxidative stress. These findings support the notion that eleutheroside E plays an anti-ferritinophagy and anti-oxidative role in HAPE. Currently, there is limited research on the efficacy evaluation of eleutheroside E treatment for HAPE. We propose that the therapeutic effect of eleutheroside E in HAPE might be attributed to its modulation of the Keap1-Nrf2 axis.

Limitations

Several limitations should be acknowledged. First, 3-MA is a broad-spectrum autophagy inhibitor that cannot definitively distinguish ferritinophagy from other autophagic processes. The potential involvement of other autophagy pathways cannot be excluded. Future studies are needed to investigate the potential involvement of macroautophagy, chaperone-mediated autophagy, or other selective autophagy pathways in this context. Second, while our data demonstrate bidirectional interaction between ferritinophagy and ferroptosis, the temporal and causal hierarchy remains to be elucidated and requires time-resolved analyses. Third, eleutheroside E was administered intraperitoneally to ensure reliable absorption under acute hypoxia, but this route does not reflect clinical practice where oral or inhaled administration would be more feasible. Oral absorption may be compromised by hypoxia-induced gastrointestinal dysfunction, while inhaled delivery requires formulation optimization.

Fourth, this study was conducted in a rat model, and caution should be exercised when extrapolating to humans. Fifth, the exact mechanisms by which eleutheroside E modulates the Keap1–Nrf2 pathway remain unclear and require further in vitro studies with gene silencing or knockout approaches. Sixth, the precise interplay between aquaporin function, barrier disruption, and ferroptosis warrants additional investigation. Collectively, these limitations do not detract from the primary findings but highlight important directions for future investigation.

Conclusion

In summary, the study reported that eleutheroside E has potential therapeutic effects against HAPE by suppressing ferritinophagy-mediated ferroptosis through the Keap1-Nrf2 axis. While the extensive crosstalk and interaction between autophagy and ferroptosis in HAPE remains unclear, our current study indicated ferroptosis as an autophagy-driven cell death process. This study provided new insights into the extreme plateau environment-related diseases, contributing towards incorporating anti-ferritinophagy and anti-ferroptosis strategies in the therapy of HAPE.

Abbreviations

AQP1, aquaporin 1; AQP4, aquaporin 4; BALF, bronchoalveolar lavage fluid; FTH1, ferritin heavy chain 1; GPX4, glutathione peroxidase 4; GSH, glutathione; HAPE, high altitude pulmonary edema; Hb, hemoglobin; HCO3, bicarbonate; Hct, hematocrit; HIF-1α, hypoxia-inducible factor-1α; HO-1, heme oxygenase-1; H&E, hematoxylin and eosin; IL-6, interleukin-6; Nrf2, Nuclear factor E2-related factor 2; Keap1, kelch-like ECH-associated protein 1; MDA, malondialdehyde; NCOA4, nuclear receptor coactivator 4; NF-κB, nuclear factor-κB; PaCO2, partial pressure of carbon dioxide; PaO2, partial pressure of oxygen; PBS, phosphate buffered saline; ROS, reactive oxygen species; SaO2, arterial oxygen saturation; SLC7A11, solute carrier family 7 member 1; SQSTM1, sequestosome1; TEM, transmission electron microscopy; TFRC, transferrin receptor; TNF-α, tumor necrosis factor-α; VEGF, vascular endothelial growth factor; W/D, wet-to-dry; HNE, 4-hydroxynonenal.

Data Sharing Statement

The datasets used and/or analysed during the current study available from the corresponding author on reasonable request.

Ethics Approval

The study protocol was approved by the Ethics Committee of Chengdu University of Traditional Chinese Medicine (Grant No. 2022-18).

Author Contributions

Yilan Wang: Conceptualization, Data curation, Formal analysis, Investigation, Methodology, Writing-original draft, Writing-review & editing, Project administration, Funding acquisition, Resources, Supervision. Nan Jia: Formal analysis, Investigation, Methodology, Visualization, Validation, Writing-original draft. Zherui Shen: Data curation, Investigation, Methodology. Sijing Zhao: Methodology, Writing-original draft. Caixia Pei: Data curation, Formal analysis. Demei Huang: Software, Data curation. Zhenxing Wang: Data curation, Formal analysis, Writing-review & editing. All authors took part in drafting, revising or critically reviewing the article; gave final approval of the version to be published; have agreed on the journal to which the article has been submitted; and agree to be accountable for all aspects of the work.

Funding

This study was financially supported by the National Natural Science Foundation of China (No. 82505498) and Sichuan Provincial Department of Science and Technology (2025ZNSFSC1852). The funder was not involved in the design of the study, nor were they engaged in collection, management, analysis, data interpretation, report writing, or the decision to submit the report for publication.

Disclosure

All authors state that they have no conflicts of interest regarding the publication of this paper.

References

1. Bärtsch P, Mairbäurl H, Maggiorini M, et al. Physiological aspects of high-altitude pulmonary edema. *Journal of Applied Physiology*. 2005;98(3):1101–1110. doi:10.1152/japplphysiol.01167.2004
2. Schoene RB. Illnesses at high altitude. *Chest*. 2008;134(2):402–416. doi:10.1378/chest.07-0561
3. Wu T, Ding S, Liu J, et al. Ataxia: an early indicator in high altitude cerebral edema. *High Altitude Medicine & Biology*. 2006;7(4):275–280. doi:10.1089/ham.2006.7.275
4. Luks AM, Auerbach PS, Freer L, et al. Wilderness Medical Society Clinical Practice Guidelines for the Prevention and Treatment of Acute Altitude Illness: 2019 Update. *Wilderness & Environmental Medicine*. 2019;30(4s):S3–s18. doi:10.1016/j.wem.2019.04.006
5. Dodson M, Castro-Portuguez R, Zhang DD. NRF2 plays a critical role in mitigating lipid peroxidation and ferroptosis. *Redox Biology*. 2019;23:101107. doi:10.1016/j.redox.2019.101107
6. Wu L, Xu W, Li H, et al. Vitamin C Attenuates Oxidative Stress, Inflammation, and Apoptosis Induced by Acute Hypoxia through the Nrf2/Keap1 Signaling Pathway in Gibel Carp (Carassius gibelio). *Antioxidants*. 2022;11(5):935. doi:10.3390/antiox11050935
7. Xin X, Li Y, Liu H. Hesperidin ameliorates hypobaric hypoxia-induced retinal impairment through activation of Nrf2/HO-1 pathway and inhibition of apoptosis. *Scientific Reports*. 2020;10(1):19426. doi:10.1038/s41598-020-76156-5
8. Ren J, Li J, Hu J, et al. Overexpression of CKIP-1 alleviates hypoxia-induced cardiomyocyte injury by up-regulating Nrf2 antioxidant signaling via Keap1 inhibition. *Biochimie*. 2019;163:163–170. doi:10.1016/j.biochi.2019.06.008
9. Dixon SJ, Lemberg KM, Lamprecht MR, et al. Ferroptosis: an iron-dependent form of nonapoptotic cell death. *Cell*. 2012;149(5):1060–1072. doi:10.1016/j.cell.2012.03.042
10. Yang X, Yang Y, Gao F, et al. N-Acetyl Serotonin Provides Neuroprotective Effects by Inhibiting Ferroptosis in the Neonatal Rat Hippocampus Following Hypoxic Brain Injury. *Molecular Neurobiology*. 2023;60(11):6307–6315. doi:10.1007/s12035-023-03464-y
11. Yi J, Zhu M, Qiu F, et al. TNFAIP1 Mediates Formaldehyde-Induced Neurotoxicity by Inhibiting the Akt/CREB Pathway in N2a Cells. *Neurotox Res*. 2020;38(1):184–198. doi:10.1007/s12640-020-00199-9
12. Wang X, Sun H, Cui L, et al. Acute high-altitude hypoxia exposure causes neurological deficits via formaldehyde accumulation. *CNS Neurosci Ther*. 2022;28(8):1183–1194. doi:10.1111/cns.13849
13. Fandrey J, Gorr T, Gassmann M. Regulating cellular oxygen sensing by hydroxylation. *Cardiovasc Res*. 2006;71(4):642–651. doi:10.1016/j.cardiores.2006.05.005
14. Zhang Y, Fang J, Dong Y, et al. High-Altitude Hypoxia Exposure Induces Iron Overload and Ferroptosis in Adipose Tissue. *Antioxidants*. 2022;11(12). doi:10.3390/antiox11122367
15. Chen LD, Wu RH, Huang YZ, et al. The role of ferroptosis in chronic intermittent hypoxia-induced liver injury in rats. *Sleep & Breathing = Schlaf & Atmung*. 2020;24(4):1767–1773. doi:10.1007/s11325-020-02091-4
16. Liu T, Wang L, Wang Q, et al. Baicalein ameliorates high-altitude hypoxic lung injury via macrophage polarization remodeling by downregulating ALOX15 pathway in ferroptosis. *Int Immunopharmacol*. 2026;168(Pt 1):115767. doi:10.1016/j.intimp.2025.115767
17. Geng Y, Hu Y, Wang H, et al. Reduced iron bioavailability drives acute high-altitude lung injury through HIF1α activation and mitophagy. *Mol Med Rep*. 2025;32(2). doi:10.3892/mmr.2025.13580

18. Wu Z, Xi Q, Zhao Q, et al. Gdf11 Overexpression Alleviates Sepsis-Induced Lung Microvascular Endothelial Barrier Damage By Activating Sirt1/Nox4 Signaling To Inhibit Ferroptosis. *Shock (Augusta, Ga)*. 2024;62(2):245–254. doi:10.1097/shk.0000000000002391
19. Quiles Del Rey M, Mancias JD. NCOA4-Mediated Ferritinophagy: a Potential Link to Neurodegeneration. *Front Neurosci*. 2019;13:238. doi:10.3389/fnins.2019.00238
20. Ito J, Omiya S, Rusu MC, et al. Iron derived from autophagy-mediated ferritin degradation induces cardiomyocyte death and heart failure in mice. *eLife*. 2021;10. doi:10.7554/eLife.62174
21. Packer M. How can sodium-glucose cotransporter 2 inhibitors stimulate erythrocytosis in patients who are iron-deficient? Implications for understanding iron homeostasis in heart failure. *Eur J Heart Fail*. 2022;24(12):2287–2296. doi:10.1002/ejhf.2731
22. Jia N, Shen Z, Zhao S, et al. Eleutheroside E from pre-treatment of Acanthopanax senticosus (Rupr.etMaxim.) Harms ameliorates high-altitude-induced heart injury by regulating NLRP3 inflammasome-mediated pyroptosis via NLRP3/caspase-1 pathway. *International Immunopharmacology*. 2023;121:110423. doi:10.1016/j.intimp.2023.110423
23. Yang X, Wang Y, Gao G. High glucose induces rat mesangial cells proliferation and MCP-1 expression via ROS-mediated activation of NF-κB pathway, which is inhibited by eleutheroside E. *J Recept Signal Transduct Res*. 2016;36(2):152–157. doi:10.3109/10799893.2015.1061002
24. Huang D, Hu Z, Yu Z. Eleutheroside B or E enhances learning and memory in experimentally aged rats. *Neural Regeneration Research*. 2013;8(12):1103–1112. doi:10.3969/j.issn.1673-5374.2013.12.005
25. Shi J, Liu Z, Li M, et al. Polysaccharide from Potentilla anserina L ameliorate pulmonary edema induced by hypobaric hypoxia in rats. *Biomed Pharmacother*. 2021;139:111669. doi:10.1016/j.biopha.2021.111669
26. Ma J, Wang C, Sun Y, et al. Comparative study of oral and intranasal puerarin for prevention of brain injury induced by acute high-altitude hypoxia. *Int J Pharm*. 2020;591:120002. doi:10.1016/j.ijpharm.2020.120002
27. Pei C, Wang F, Huang D, et al. Astragaloside IV protects from PM2.5-induced lung injury by regulating autophagy via inhibition of PI3K/Akt/mTOR signaling in vivo and in vitro. *Journal of Inflammation Research*. 2021;14:4707–4721. doi:10.2147/jir.S312167
28. Wang Y, Shen Z, Zhao S, et al. Sipeimine ameliorates PM2.5-induced lung injury by inhibiting ferroptosis via the PI3K/Akt/Nrf2 pathway: a network pharmacology approach. *Ecotoxicology and Environmental Safety*. 2022;239:113615. doi:10.1016/j.ecoenv.2022.113615
29. Wang Y, Shen Z, Pei C, et al. Eleutheroside B ameliorated high altitude pulmonary edema by attenuating ferroptosis and necroptosis through Nrf2-antioxidant response signaling. *Biomed Pharmacother*. 2022;156:113982. doi:10.1016/j.biopha.2022.113982
30. Pei C, Shen Z, Wu Y, et al. Eleutheroside B Pretreatment Attenuates Hypobaric Hypoxia-Induced High-Altitude Pulmonary Edema by Regulating Autophagic Flux via the AMPK/mTOR Pathway. *Phytotherapy Research: PTR*. 2024;38(12):5657–5671. doi:10.1002/ptr.8333
31. Matute-Bello G, Winn RK, Jonas M, et al. Fas (CD95) induces alveolar epithelial cell apoptosis in vivo: implications for acute pulmonary inflammation. *The American Journal of Pathology*. 2001;158(1):153–161. doi:10.1016/s0002-9440(10)63953-3
32. Fang Y, Chen X, Tan Q, et al. Inhibiting Ferroptosis through Disrupting the NCOA4-FTH1 Interaction: a New Mechanism of Action. *ACS Central Science*. 2021;7(6):980–989. doi:10.1021/acscentsci.0c01592
33. Guan D, Zhou W, Wei H, et al. Ferritinophagy-Mediated Ferroptosis and Activation of Keap1/Nrf2/HO-1 Pathway Were Conducive to EMT Inhibition of Gastric Cancer Cells in Action of 2,2'-Di-pyridineketone Hydrazone Dithiocarbamate Butyric Acid Ester. *Oxidative Medicine and Cellular Longevity*. 2022;2022:3920664. doi:10.1155/2022/3920664
34. West JB. High-altitude medicine. *The Lancet Respiratory Medicine*. 2015;3(1):12–13. doi:10.1016/s2213-2600(14)70238-3
35. Wang S, Yang X. Eleutheroside E decreases oxidative stress and NF-κB activation and reprograms the metabolic response against hypoxia-reoxygenation injury in H9c2 cells. *International Immunopharmacology*. 2020;84:106513. doi:10.1016/j.intimp.2020.106513
36. Fukada K, Kajiya-Sawane M, Matsumoto Y, et al. Antiedema effects of Siberian ginseng in humans and its molecular mechanism of lymphatic vascular function in vitro. *Nutr Res*. 2016;36(7):689–695. doi:10.1016/j.nutres.2016.02.012
37. Zhang XL, Ren F, Huang W, et al. Anti-fatigue activity of extracts of stem bark from Acanthopanax senticosus. *Molecules (Basel, Switzerland)*. 2010;16(1):28–37. doi:10.3390/molecules16010028
38. Mishra KP, Sharma N, Soree P, et al. Hypoxia-Induced Inflammatory Chemokines in Subjects with a History of High-Altitude Pulmonary Edema. *Indian J Clin Biochem*. 2016;31(1):81–86. doi:10.1007/s12291-015-0491-3
39. Foster MW, Thompson JW, Que LG, et al. Proteomic analysis of human bronchoalveolar lavage fluid after subsgemental exposure. *Journal of Proteome Research*. 2013;12(5):2194–2205. doi:10.1021/pr400066g
40. Hanaoka M, Kobayashi T, Droma Y, et al. Clinical and Pathophysiological Features of High-altitude Pulmonary Edema in the Japanese Population: a Review of Studies on High-altitude Pulmonary Edema in Japan. *Internal medicine (Tokyo, Japan)*. 2024;63(17):2355–2366. doi:10.2169/internalmedicine.2533-23
41. Bratke K, Weise M, Stoll P, et al. Flow Cytometry as an Alternative to Microscopy for the Differentiation of BAL Fluid Leukocytes. *Chest*. 2024;166(4):793–801. doi:10.1016/j.chest.2024.03.037
42. Thi Nghiem TH, Kusuma F, Park J, et al. Brief guide to detecting ferroptosis. *Mol Cells*. 2025;48(11):100276. doi:10.1016/j.mocell.2025.100276
43. Zhang S, Liu J, Jiang D, et al. The plasma level changes of VEGF and soluble VEGF receptor-1 are associated with high-altitude pulmonary edema. *J Med Invest*. 2018;65(1.2):64–68. doi:10.2152/jmi.65.64
44. Tanaka T, Narazaki M, Kishimoto T. IL-6 in inflammation, immunity, and disease. *Cold Spring Harb Perspect Biol*. 2014;6(10):a016295. doi:10.1101/cshperspect.a016295
45. Blaser H, Dostert C, Mak TW, et al. TNF and ROS Crosstalk in Inflammation. *Trends in Cell Biology*. 2016;26(4):249–261. doi:10.1016/j.tcb.2015.12.002
46. Zhou Q, Wang D, Liu Y, et al. Solnatide Demonstrates Profound Therapeutic Activity in a Rat Model of Pulmonary Edema Induced by Acute Hypobaric Hypoxia and Exercise. *Chest*. 2017;151(3):658–667. doi:10.1016/j.chest.2016.10.030
47. Woods P, Alcock J. High-altitude pulmonary edema. *Evolution, Medicine, and Public Health*. 2021;9(1):118–119. doi:10.1093/emph/eoaa052
48. Tsai MC, Lin HJ, Lin MT, et al. High-altitude pulmonary edema can be prevented by heat shock protein 70-mediated hyperbaric oxygen preconditioning. *The Journal of Trauma and Acute Care Surgery*. 2014;77(4):585–591. doi:10.1097/ta.0000000000000408
49. Grocott MP, Martin DS, Levett DZ, et al. Arterial blood gases and oxygen content in climbers on Mount Everest. *N Engl J Med*. 2009;360(2):140–149. doi:10.1056/NEJMoa0801581
50. Lee JW, Lee J, Um SH, et al. Synovial cell death is regulated by TNF-α-induced expression of B-cell activating factor through an ERK-dependent increase in hypoxia-inducible factor-1α. *Cell Death & Disease*. 2017;8(4):e2727. doi:10.1038/cddis.2017.26

51. Wang B, Hou J, Li J, et al. Low-pressure exposure influences the development of HAPE. *Open Life Sci*. 2025;20(1):20221029. doi:10.1515/biol-2022-1029
52. Vrettou CS, Issaris V, Kokkoris S, et al. Exploring Aquaporins in Human Studies: mechanisms and Therapeutic Potential in Critical Illness. *Life*. 2024;14(12). doi:10.3390/life14121688
53. Tan J, Gao C, Wang C, et al. Expression of Aquaporin-1 and Aquaporin-5 in a Rat Model of High-Altitude Pulmonary Edema and the Effect of Hyperbaric Oxygen Exposure. *Dose Response*. 2020;18(4):1559325820970821. doi:10.1177/1559325820970821
54. Zhang X, Ma X, Li Y, et al. Dexamethasone Upregulates the Expression of Aquaporin4 by Increasing SUMOylation in A549 Cells. *Inflammation*. 2020;43(5):1925–1935. doi:10.1007/s10753-020-01267-0
55. Sies H, Jones DP. Reactive oxygen species (ROS) as pleiotropic physiological signalling agents. *Nature Reviews Molecular Cell Biology*. 2020;21(7):363–383. doi:10.1038/s41580-020-0230-3
56. Xiao M, Zhong H, Xia L, et al. Pathophysiology of mitochondrial lipid oxidation: role of 4-hydroxynonenal (4-HNE) and other bioactive lipids in mitochondria. *Free Radical Biology & Medicine*. 2017;111:316–327. doi:10.1016/j.freeradbiomed.2017.04.363
57. Tsikas D. Assessment of lipid peroxidation by measuring malondialdehyde (MDA) and relatives in biological samples: analytical and biological challenges. *Analytical Biochemistry*. 2017;524:13–30. doi:10.1016/j.ab.2016.10.021
58. Tsai SH, Huang PH, Tsai HY, et al. Roles of the hypoximir microRNA-424/322 in acute hypoxia and hypoxia-induced pulmonary vascular leakage. *FASEB Journal*. 2019;33(11):12565–12575. doi:10.1096/fj.201900564RR
59. Remillard CV, Yuan JX. High altitude pulmonary hypertension: role of K+ and Ca2+ channels. *High Altitude Medicine & Biology*. 2005;6(2):133–146. doi:10.1089/ham.2005.6.133
60. Zhao Z, Hou B, Tang L, et al. High-altitude hypoxia-induced rat alveolar cell injury by increasing autophagy. *Int J Exp Pathol*. 2022;103(4):132–139. doi:10.1111/iep.12434
61. Stockwell BR, Friedmann Angeli JP, Bayir H, et al. Ferroptosis: a Regulated Cell Death Nexus Linking Metabolism, Redox Biology, and Disease. *Cell*. 2017;171(2):273–285. doi:10.1016/j.cell.2017.09.021
62. Zhao CQ, Wang C, Liu MM, et al. Single-cell transcriptomes reveal heterogeneity of chlorine-induced mice acute lung injury and the inhibitory effect of pentoxifylline on ferroptosis. *Sci Rep*. 2023;13(1):6833. doi:10.1038/s41598-023-32093-7
63. Usatyuk PV, Parinandi NL, Natarajan V. Redox regulation of 4-hydroxy-2-nonenal-mediated endothelial barrier dysfunction by focal adhesion, adherens, and tight junction proteins. *The Journal of Biological Chemistry*. 2006;281(46):35554–35566. doi:10.1074/jbc.M607305200
64. Wen Q, Liu J, Kang R, et al. The release and activity of HMGB1 in ferroptosis. *Biochem Biophys Res Commun*. 2019;510(2):278–283. doi:10.1016/j.bbrc.2019.01.090
65. Wang Y, Wang M, Liu Y, et al. Integrated regulation of stress responses, autophagy and survival by altered intracellular iron stores. *Redox Biol*. 2022;55:102407. doi:10.1016/j.redox.2022.102407
66. Jiang Y, Liu X, Sun M. The mist of ferroptosis: the Orpheus journey of mitochondria - Exploring the symphony of cell fate. *Int J Biol Macromol*. 2025;319(Pt 2):145472. doi:10.1016/j.ijbiomac.2025.145472
67. Mizushima N, Komatsu M. Autophagy: renovation of cells and tissues. *Cell*. 2011;147(4):728–741. doi:10.1016/j.cell.2011.10.026
68. Wu Z, Geng Y, Lu X, et al. Chaperone-mediated autophagy is involved in the execution of ferroptosis. *Proc Natl Acad Sci U S A*. 2019;116(8):2996–3005. doi:10.1073/pnas.1819728116
69. Bai Y, Meng L, Han L, et al. Lipid storage and lipophagy regulates ferroptosis. *Biochem Biophys Res Commun*. 2019;508(4):997–1003. doi:10.1016/j.bbrc.2018.12.039
70. Lisk C, Mccord J, Bose S, et al. Nrf2 activation: a potential strategy for the prevention of acute mountain sickness. *Free Radical Biology & Medicine*. 2013;63:264–273. doi:10.1016/j.freeradbiomed.2013.05.024
71. Li X, Sung P, Zhang D, et al. Curcumin in vitro Neuroprotective Effects Are Mediated by p62/keap-1/Nrf2 and PI3K/AKT Signaling Pathway and Autophagy Inhibition. *Physiol Res*. 2023;72(4):497–510.
72. Emmanuel N, Li H, Chen J, et al. FSP1, a novel KEAP1/NRF2 target gene regulating ferroptosis and radioresistance in lung cancers. *Oncotarget*. 2022;13:1136–1139. doi:10.18632/oncotarget.28301
73. Anandhan A, Dodson M, Shakya A, et al. NRF2 controls iron homeostasis and ferroptosis through HERC2 and VAMP8. *Science Advances*. 2023;9(5):eade9585. doi:10.1126/sciadv.ade9585
74. Kong L, Deng J, Zhou X, et al. Sitagliptin activates the p62-Keap1-Nrf2 signalling pathway to alleviate oxidative stress and excessive autophagy in severe acute pancreatitis-related acute lung injury. *Cell Death & Disease*. 2021;12(10):928. doi:10.1038/s41419-021-04227-0
75. Yang J, Mo J, Dai J, et al. Cetuximab promotes RSL3-induced ferroptosis by suppressing the Nrf2/HO-1 signalling pathway in KRAS mutant colorectal cancer. *Cell Death & Disease*. 2021;12(11):1079. doi:10.1038/s41419-021-04367-3
76. Koppula P, Zhuang L, Gan B. Cystine transporter SLC7A11/xCT in cancer: ferroptosis, nutrient dependency, and cancer therapy. *Protein & Cell*. 2021;12(8):599–620. doi:10.1007/s13238-020-00789-5
77. Wang G, Qin S, Zheng Y, et al. T-2 Toxin Induces Ferroptosis by Increasing Lipid Reactive Oxygen Species (ROS) and Downregulating Solute Carrier Family 7 Member 11 (SLC7A11). *J Agric Food Chem*. 2021;69(51):15716–15727. doi:10.1021/acs.jafc.1c05393
78. Mesquita G, Silva T, Gomes AC, et al. H-Ferritin is essential for macrophages' capacity to store or detoxify exogenously added iron. *Scientific Reports*. 2020;10(1):3061. doi:10.1038/s41598-020-59898-0
79. Yu H, Chen B, Ren Q. Baicalin relieves hypoxia-aroused H9c2 cell apoptosis by activating Nrf2/HO-1-mediated HIF1α/BNIP3 pathway. *Artificial Cells, Nanomedicine, and Biotechnology*. 2019;47(1):3657–3663. doi:10.1080/21691401.2019.1657879